

Analysis of dynamic light scattering signals with discrete wavelet transformation

M. KROON(*), G. H. WEGDAM and R. SPRIK

*Van der Waals-Zeeman Instituut, Universiteit van Amsterdam
Valckenierstraat 65, 1018 XE Amsterdam, The Netherlands*

(received 25 March 1996; accepted in final form 12 July 1996)

PACS. 78.35+c – Brillouin and Rayleigh scattering.

PACS. 05.40+j – Fluctuation phenomena, random processes, and Brownian motion.

PACS. 02.70–c – Computational techniques.

Abstract. – The analysis of non-stationary signals calls for specific tools which go beyond classical Fourier analysis. Here we present the discrete wavelet transform as a quantitative method to analyse the scaling properties of non-stationary and chaotic signals obtained by light scattering. The analysis is performed directly on the time-resolved scattered intensity. The result is the scaling exponent of the underlying power spectrum and the frequency window where the scaling can be observed. These properties are obtained with a higher accuracy and in a fraction of the time compared with the classical method of intensity correlation functions. As a test we applied the new method to the sol-gel transition of a suspension of disc-shaped colloidal particles in water.

A classical tool for spectral analysis of recorded signal traces is the Fourier transform as devised by Fourier in 1822 [1]. Fourier analysis is ideal for analysing stationary periodic signals. However, it fails when processing non-stationary signals because frequency information is extracted for the complete duration of the measured signal. A possible solution to study local spectral properties is offered by the windowed Fourier transform [2]. The analysis introduces a scale, namely the width of the window. Still the windowed Fourier transform fails when processing strongly chaotic signals. The basic flaw is the use of harmonic waves as analysing functions, local in frequency but completely delocalized in time, or *vice versa*. Clearly, there exists the need for an analysis which processes signals locally in time without any prejudice to scale, which can handle non-stationary and chaotic signals, which show self-similar behaviour. Wavelet analysis [2], [3] has proven to be the natural tool to handle such signals. In the context of dynamical systems, wavelet analysis is able to reveal the successive fractal branching characteristic of self-similar invariant measures on strange attractors [4]. Due to their ability to detect singularities, wavelets were then applied to the analysis of turbulence data [5].

The analysing wavelet functions are constructed from a single function, the *mother wavelet*, by dilations and translations. Within the constraints imposed they are localized in time as well

(*) E-mail: kroon@phys.uva.nl.

as in frequency space. In the analysis, the width of the analysing wavelet varies logarithmically rather than linearly. Wavelets provide us with a mathematical microscope, able to analyse the local scaling behaviour of signals. Here we report on the novel application of the discrete wavelet transform [3], or wavelet-based multiresolution analysis, on signals obtained from dynamic light scattering experiments. In these experiments, the intensity correlation functions are observed to show a power law decay over many decades in time [6]-[9]. Hence their Fourier transform, the power spectrum of intensity fluctuations, shows scaling with frequency. For a physical interpretation of the process studied in these examples it is essential to prove the power law decay, to determine the range over which it extends, and the exponent of the decay. The signals measured in the examples possess all these characteristics. In this paper we will show that the relevant information can be obtained in a direct and fast way by a wavelet-based multiresolution analysis. First we will treat the basics of wavelet analysis, then the application to light scattering experiments. Finally we discuss the relevance of our findings.

The original impetus for wavelets came from the analysis of earthquake records [10], but wavelet analysis has found important applications in turbulence analysis [5], speech and image processing, and is now a significant tool in signal analysis in general. One begins by defining a (complex-valued) window function $\Psi(t)$ which is called the *mother wavelet*. The continuous wavelet transformation of a measured signal $f(t)$ is given by [3]

$$f(s, u) = \int_{-\infty}^{+\infty} f(t) \Psi\left(\frac{t-u}{s}\right) dt, \quad (1)$$

where s is the scale/dilation factor and u is the translation parameter. Time localization is achieved by “looking” at the signal through translated versions of the analysing function. The local frequency information is extracted as a function of the scaling parameter s , which determines the scale of fluctuations being analysed.

The continuous formulation of the wavelet transform is however not very useful for discretely sampled signals. Around 1986 a new method for performing wavelet analysis on discrete signals was developed by Mallat, known as discrete wavelet transformation (DWT) [3, 11]. This method is completely recursive and therefore ideal for computations [12]. We start with a discretely sampled trace $I^{(0)}(n)$ of length $K_0 = 2^M$ on the finest scale t_0 , where time is replaced with $n \cdot t_0$. The trace is now split up into a *blurred* approximation $I^{(1)}$ and the removed *detail* $d^{(1)}$ on the coarser scale $\tau_1 = 2^1 \cdot t_0$. The latter contains all fluctuations of scale t_0 which can no longer be represented on the coarser scale τ_1 . Recursive application builds a hierarchy of approximations $I^{(0)}, I^{(1)}, \dots, I^{(p)}$ on coarsening scales $\tau_p = 2^p \cdot t_0$, accompanied by the removed *detail* $d^{(p)}$.

In the formal definitions of Mallat’s algorithm the traces $I^{(p)}$ are expanded on the basis of orthonormal wavelet functions $\Psi_{p,k}$ according to $I^{(p)} = \sum_k I^{(p)}(k) \Psi_{p,k}$. The family of functions $\Psi_{p,k}(t) = 2^{-p/2} \Psi(2^{-p} t - k)$ are scaled and translated versions of the *mother wavelet* $\Psi(t)$, for which $\langle \Psi_{p,k} | \Psi_{p,m} \rangle \equiv \int dt \Psi_{p,k}(t) \Psi_{p,m}(t) = 0$ holds for $k \neq m$. The transformation of $I^{(p)}$ into $I^{(p+1)}$ is achieved by an averaging procedure,

$$I^{(p+1)}(m) = \sum_{k=0}^{K_p-1} w(k-2m) I^{(p)}(k), \quad m = 0, \dots, K_{p+1}, \quad (2)$$

where $w(k-2m) = \langle \Psi_{p+1,m} | \Psi_{p,k} \rangle$, $K_p = 2^{M-p}$, and time is represented by $m \cdot \tau_{p+1}$. The operation, which is basically a matrix product, reduces the number of data points K_p with a factor 2, since the resulting trace “lives” on a twice as large scale. The resulting loss of

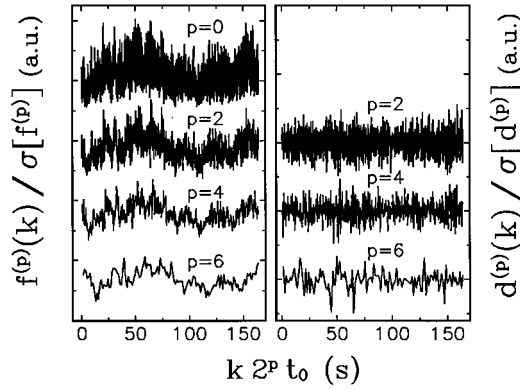


Fig. 1. – The result of subsequent discrete wavelet transformations on a measured intensity trace (l.h.s.) and the removed *detail* (r.h.s.), where time is represented by $k \cdot 2^p \cdot t_0$. The results are normalized with respect to the width σ of the distribution. We plot only even p for convenience. Note that the structure of the self-similar trace remains conserved.

information, expressed in the removed *detail* $d^{(p+1)}$ on the scale τ_p , can be found by

$$d^{(p+1)}(m) = \sum_{k=0}^{K_p-1} g(k-2m) I^{(p)}(k) , \quad m = 0, \dots, K_{p+1} , \quad (3)$$

where the filter coefficients $g(n)$ and $w(n)$ are related via $g(n) = (-1)^n w(1-n)$, the quadrature mirror filter constraint.

As analysing functions Ψ we use the Daubechies wavelets [2, 3, 11]. With these specific functions the number of non-zero filter coefficients $w(n)$ is limited, and equal to the order N ($= 4, 6, 8, \dots$) of the Daubechies wavelet. Besides their ability to form an orthonormal basis of compactly supported wavelets with as much locality and smoothness as desired, they are constructed such that the moments $\langle x^m \rangle \equiv \int x^m \Psi(x) dx = 0$ for $m = 0, \dots, N-1$, one of the reasons for the popularity of these wavelets. We refer the interested reader to the excellent book by Newman [11] for a clear introduction to the Daubechies wavelets.

The analysis now proceeds via the removed *detail* $d^{(p)}(k)$. The variance and higher moments of $d^{(p)}(k)$ represent the moments of the distribution of fluctuations on the scale τ_p [13]. If the spectral density $S(\omega)$ of the signal fluctuations shows scaling, *i.e.* $S(\omega) \sim \omega^{-\gamma}$, then DWT reveals this scaling through the variance $\sigma^2\{d^{(p)}\}$ as a function of τ_p by

$${}^2 \log(\sigma^2\{d^{(p)}\}) = {}^2 \log(\sigma^2) + \gamma^2 \log(\tau_p/t_0) , \quad (4)$$

known as the variance progression [13]. Here σ^2 is the variance of $I(n)$ sampled on the finest scale t_0 . The signal processing carried out with eqs. (2) and (3) conserves the true moments of the sampled signal, since the contribution of the wavelet function to the moments equals zero.

In our experiment we measure time-resolved recordings of the fluctuating scattered intensity during the gelation process of a suspension of anisotropic monodisperse colloidal discs, called Laponite, in water. A detailed account of an extended dynamic light scattering study of the Laponite system can be found elsewhere [9]. The trace $I(n)$ is sampled with a gate-time $t_0 = 20$ ms in blocks of $K_0 = 2^{15}$ discrete sampling points. The recorded trace can be considered stationary on a time scale of minutes, which is sufficient to characterize the

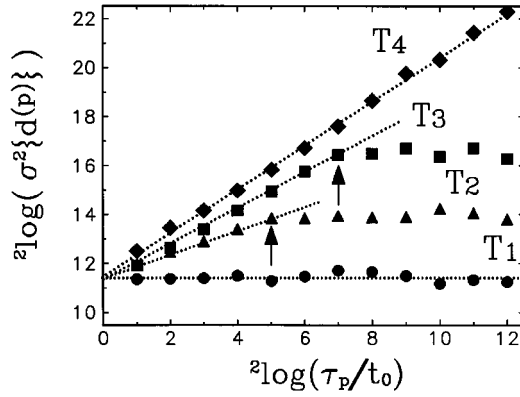


Fig. 2. – The variance $\sigma^2\{d^{(p)}\}$ vs. the scale τ_p on a double-logarithmic scale. The symbols T_i denote well-separated regions in the gelation process and are related to the T_i symbols in fig. 3. The arrows indicate the scale τ'_p where $\sigma^2\{d^{(p)}\}$ deviates from the straight-line behaviour (dotted lines).

spectrum. We recursively apply DWT to one block, as shown partially in fig. 1, where we limit $p \leq 12$ to warrant statistical accuracy. The self-similar structure of the measured trace remains conserved although frequency components higher than $\omega_p = \tau_p^{-1}$ are stripped off. Results obtained with different Daubechies wavelet order N are remarkably similar. Therefore, we limit the discussion to $N = 12$.

In fig. 2 we plot $\sigma^2\{d^{(p)}\}$ vs. τ_p , obtained from measurements of the trace $I(n)$ at well-separated regions T_i of the gelation process. Just after sample preparation (region T_1) the $\sigma^2\{d^{(p)}\}$ curve is flat over the entire time range covered. In region T_2 we observe the first few points of the curve to lie on a straight line which breaks off at a certain scale τ'_p , denoted by arrows in fig. 2. Beyond this (time) scale, or below its inverse (frequency) scale $\omega'_p = (\tau'_p)^{-1}$, the algebraic scaling ceases. As the gelation proceeds we observe the slope γ and the range τ'_p of the scaling part to increase as shown in fig. 3 and 4. Finally, in the gel (region T_4) we observe a scaling over the entire time range $2^{15} t_0 = 655$ s of the trace. Here γ has settled at a relatively constant value 0.86 ± 0.04 .

In fig. 4 we show τ'_p vs. the normalized distance $\epsilon = (T_g - T)/T_g$ to the gel-point T_g , where $T_g = 100$ hours [9]. Approaching T_g we observe τ'_p to “stretch” to infinity according to $\tau'_p \sim \epsilon^\phi$, where the critical exponent $\phi = -3.3 \pm 0.2$. Due to the restricted time duration of the recorded trace, the stretching of τ'_p is followed over a limited range in p . Measurement of the intensity trace using a different gate-time tends to shift the results as shown in fig. 3 and 4 with respect to the horizontal axis only. Therefore the scale τ'_p is the characteristic (time) scale in the development of the gel, and the scaling exponent γ defines the state of the suspension in the process of gelation.

For an assessment of these results it is important to note that in region T_1 and subsequently beyond the scale τ'_p the algebraic scaling ceases. In the classical method of dynamic light scattering we would have observed an exponentially decaying tail in the correlation function, or a Lorentzian spectral density. The correctness of this interpretation is beared out by extensive simulations, done by us along the lines set out by Mandelbrot [14] and Kaplan [13]. Model spectra yielding other than algebraic correlations show continuous deviation from the straight-line behaviour in the double-logarithmic plot of variance vs. scale. Wavelet analysis discriminates between exponential, stretched exponential and algebraic decay. The experimental results on the gel-phase are obtained assuming the scattered signal is not mixed

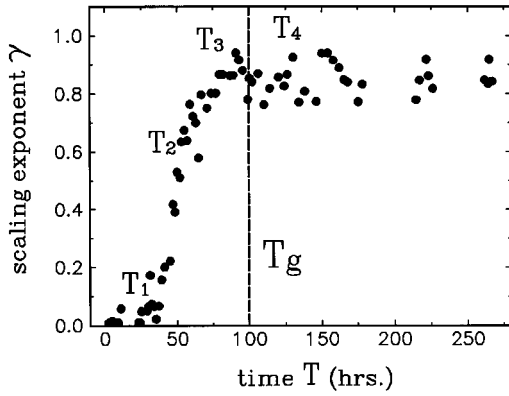


Fig. 3.

Fig. 3. – The scaling exponent γ of $\sigma^2\{d^{(p)}\}$ vs. τ_p , as shown in fig. 2, vs. the time T after preparation of the sample. The dashed line shows the gel point $T_g = 100$ hours [9]. In the gel-phase (region T_4) γ settles at a relatively constant value of 0.86 ± 0.04 .

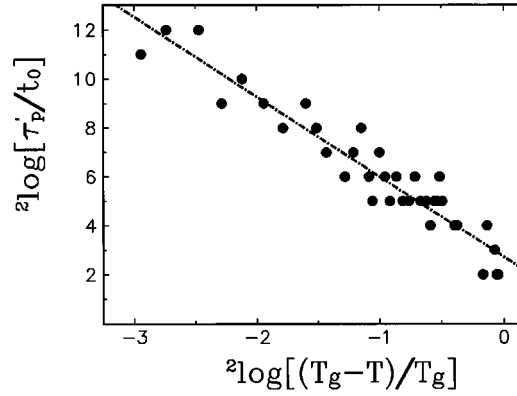


Fig. 4.

Fig. 4. – The scale τ_p' vs. the normalized distance to the gel-point $\epsilon = (T_g - T)/T_g$, where $T_g = 100$ hours. τ_p' is denoted by arrows in fig. 2. The dashed line shows a power regression fit to the data with $\tau_p' \sim \epsilon^{-3.3}$.

with a constant background scattered off the partially frozen-in gel structure [9]. However, only in the sol-phase this background is absent. The correction on γ can easily be derived from the simulations. The overall corrections are found to be small and will lead to a somewhat steeper rise in the value of γ , as shown in fig. 3.

The spectrum of the density fluctuations, which is measured by light scattering, changes continuously when the colloidal system is going through the transition. It shows an algebraically decaying part between a high- and low-frequency cut-off, the latter is approaching zero frequency at the transition. These characteristics can be addressed quantitatively with wavelet analysis and are obtained without the bias of a presupposed model to analyse the data with. With correlation functions the bias is introduced by the necessity to use a functional form, on the basis of a model or as a practical phenomenological tool, to obtain the characteristic parameters [8], [9]. Moreover, the correlation functions can be measured only with any reliability, when the evolution of the spectral distribution is a few orders slower than the inverse of the low-frequency cut-off. Wavelet analysis does not suffer from these drawbacks. It is fast and efficient and can be used as a valuable tool in analysing non-stationary signals, physical systems in non-stationary states, such as glass or gel-formation, and non-stationary processes as turbulence. It is the natural tool for fractal signals in general.

This research is part of the program supported by the Foundation for Fundamental Research of Matter (FOM) and is financially supported by the Netherlands Organization of Scientific Research (NWO).

REFERENCES

- [1] BRACEWELL R. N., *The Fourier Transform and its Applications*, 2nd edition (McGraw-Hill, New York, N.Y.) 1986.
- [2] KAISER G., *A Friendly Guide to Wavelets* (Birkhäuser, Berlin) 1994.
- [3] DAUBECHIES I., in *Wavelets, Time-Frequency Methods and Phase Space, Proceedings of the International Conference, Marseille, 1987*, edited by J. M. COMBES, A. GROSSMANN and PH. TCHAMITCHIAN (Springer-Verlag) 1989.
- [4] ARNEODO A., GRASSEAU G. and HOLSCHNEIDER M., *Phys. Rev. Lett.*, **61** (1988) 2281.
- [5] ARGOUL F., ARNEODO A., GRASSEAU G., GANGE Y., HOPFINGER E. J. and FRISCH U., *Nature*, **338** (1989) 51.
- [6] JOOSTEN J. G. H., GELADÉ E. T. F. and PUSEY P. N., *Phys. Rev. A.*, **42** (1990) 2161.
- [7] REN S. Z. and SORENSEN C. M., *Phys. Rev. Lett.*, **70** (1993) 1727.
- [8] BARTSCH E., ANTONIETTI M., SCHUPP W. and SILLESCU H., *J. Chem. Phys.*, **97** (1992) 3950.
- [9] KROON M., WEGDAM G. H. and SPRIK R., submitted to *Phys. Rev. E*.
- [10] GOUPILLAUD P., GROSSMANN A. and MORLET J., *Geoplotation*, **23** (1984) 85.
- [11] NEWMAN D. E., *Random Vibrations, Spectral and Wavelet Analysis*, 3rd edition (Wiley, New York, N.Y.) 1993.
- [12] PRESS W. H., TEUKOLSKY S. A., VETTERING W. T. and FLANNERY B. P., *Numerical Recipes in Fortran*, 2nd edition, (Cambridge, New York, N.Y.) 1992.
- [13] KAPLAN L. M. and JAY KUO C. C., *IEEE Trans. Sig. Proc.*, **41** (1993) 3554.
- [14] MANDELBROT B. M. and NESS J. W. V., *Fractional Brownian motions, fractional noises and applications*, *SIAM Rev.*, Vol. 10, October 1968.